Lanzetta, M.; Tantussi, G.; Santochi, M.: The Process Control in Manufacturing: Inspection of Ball Bearings
PRIME 2001, 1st International Seminar on: *PRogress in Innovative Manufacturing Engineering*
Ed.P.M.Lonardo, Sestri Levante (GE) Italy, June, 20th-22nd, 2001, ISBN:88-900559-0-1, p.405-410

The Process Control in Manufacturing: Inspection of Ball Bearings

M. Lanzetta, G. Tantussi, M. Santochi
Department of Mechanical, Nuclear and Production Engineering, University of Pisa, Pisa, Italy

Abstract

A real industrial case has been analyzed and is discussed in this paper. Significant percentage of defective ball bearings is not detected during the final inspection in the only manual station of the automatic assembly line. The main specifications of an inspection system, which is based on artificial vision, are pointed out. The system configuration (camera, lighting and ball bearing support) is described in detail. The visibility of all surfaces has been optimized using one central conic and four lateral mirrors. In off-line tests, the described algorithms allowed the recognition of most surface defects. Interactive and user-friendly calibration procedures have also been defined.

Keywords: Automated assembly, Quality control, Artificial vision

1 INTRODUCTION

About 60 billion ball bearings are manufactured every year all over the world for applications ranging from aerospace to machinery. The examined line output is 5000 products per shift.

For high-tech companies, the last trend is zero-defect manufacturing. For large-scale products, high investments in the process control are required to prevent defective products from reaching the market.

This study is divided in two parts:

1. the collection of rejected products and the analysis of typical defects;
2. the development and testing of an automatic inspection system.

State of the art

Artificial vision is widespread today in manufacturing [1] [2], mainly for inspection [3] [4] [5]. Several examples are available from the robotic/automatic [6] electronic [7] [8] and electrotechnical [9] assembly industry, both in 2D and in 3D [9]. Detection algorithms include artificial neural networks [7].

Regarding ball bearings, several applications have been developed for SKF [10] [11] [12], but these systems are only able to detect the absence of parts.

Specular reflection [13] [14] is a standard technique to extend the view field of a camera to surfaces that are not directly visible. The main reason for doing so is reducing the time for inspection and the need for additional handling devices. The main drawback is the consequent reduction of the spatial resolution. In this particular application the use of reflective surfaces is stressed.

The inspection of markings is a critical problem, because, in addition to integrity, it involves understanding by a human. An industrial system is described in [15].

2 THE MANUFACTURING LINE

2.1 The process control

The main parts of a ball bearing are shown in Figure 1.

From a detailed analysis of the line, the main operations (machining and assembly) and controls have been summarized in the graph of Figure 2.

The process control, certified with the ISO 9001 standards, is mainly based on the product control before and after the most critical operations. Any deviation from the correct range is monitored. Corrective measures are taken manually when noncompliance occurs.

Regarding the criticality of defects, a product should be rejected in any of the following situations:

- when a functional defect is present, e.g. rotational problems;

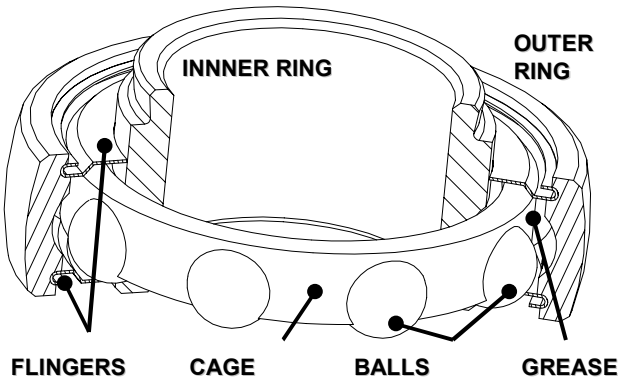

Figure 1: The main functional parts of a ball bearing (model SKF YET 208).

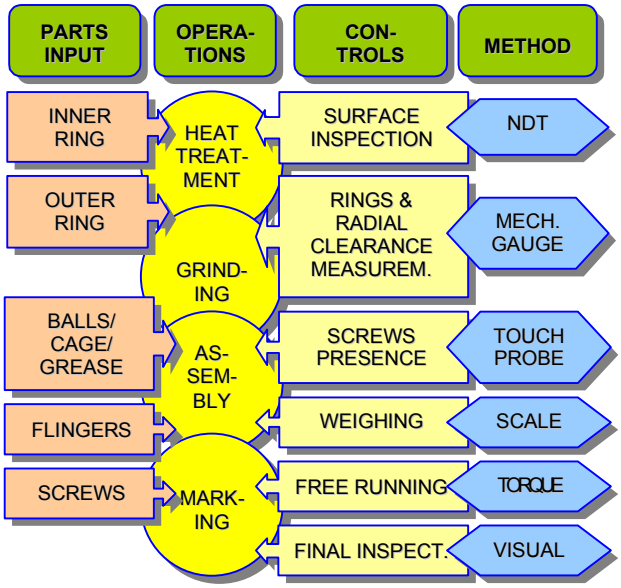

Figure 2: Sequence of the main operations (top-down) and controls performed on the ball bearings manufacturing line. The control methods are also indicated.

- for defects on the outer surface, which may affect the final product installation;
- all surface defects are critical for esthetical reasons. Visible defects are larger than about 1 mm.

Receiving inspection

The cage and the inner and outer rings are provided by ISO certified suppliers. It has been observed that about 0.1 percent of defective parts are provided, so the procurement process can be improved. Surface and other defects on these parts can be detected on the line with the controls indicated in Figure 2 and in the final visual inspection station.

Weighing

The accuracy of this control depends on the weight variability of parts and grease. Within this range, for all ball bearing models, the absence of one ball or of one flinger can be detected. The cage or the screws absence cannot be detected with this method and is checked with other automatic inspection systems (Figure 2).

Audits

In parallel with the above controls, according to the MIL standards [16], product audits based on a sampling plan are performed on final products, every week, at the end of the line. This activity allows a quantitative statistical assessment of the controls performance.

2.2 Visual inspection

The only manual control is the visual inspection of the final product at the end of the line. This operation includes:

- checking the presence of all parts;
- a functional test (manual free running control);
- the detection of esthetical or surface defects;
- the readability of markings.

The classification of visual defects on ball bearings

The ball bearing surfaces to be inspected are:

- the two lateral plane faces of the inner (IPF) and outer (OPF) rings;
- the two flingers (F);
- the inner cylindrical surface (IS);
- the outer spherical surface (OS).

An exhaustive classification of defects is reported in Table 1. Some examples are displayed in Figure 3.

Discussion

From the analysis of the data collected over a period of nine months, it has been observed that over 10% of visible defects are skipped in the visual inspection station. The first corrective action taken has been the operators awakening, but no benefits have been observed, for several reasons, including:

- the operator's capability;
- the monotony and repetitiveness of this task;
- the high production rate required.

Several alternative solutions are possible, including:

1. zero-defect suppliers;
2. automating the inspection operations.

The second alternative requires higher initial investments, but it has a lower cost in the long term and first of all it is able to provide the required performance by eliminating the human error. In the remainder, the feasibility and the specifications of such automatic inspection system are discussed.

A distributed use of artificial vision extended to previous stations would allow the detection of esthetical defects before subsequent operations are performed and more value is added to a product that will be rejected. This application requires an economical analysis.

The potential of artificial vision for inspection may include gauging. The integration of these tests (which are performed on the line with the methods indicated in Figure 2) into the final inspection station under study, requires a higher camera resolution for the tight product tolerances.

3 THE AUTOMATIC VISUAL INSPECTION STATION

The purpose of this system is to detect all the surface defects indicated in Table 1 with objective criteria and constant efficiency.

The main steps of this study are:

- finding the optimal system configuration;
- the selection of light sources and their distribution;
- the definition of algorithms.

Table 1: The classification of visible defects, their position (the abbreviations are in Chapter 2.2) and reference to the examples displayed in Figure 3. Their relative occurrence is based on quality audits monitoring the controls effectiveness over a period of nine months.

Defect Name	Position and Example Reference (Figure 3)	Relative Occurr.
TURNING MARKS	IS (h.), OS, IPF, OPF	28%
GRINDING MARKS	IS (f.), OS (d.), IPF, OPF (b.)	11%
RUST TRACES	IS (g.), OS, IPF (g), OPF	38%
HAMMERING	F (c.)	20%
BLOT	F (a.)	3%
UNREADABLE MARKING	IPF (ON 1 SIDE ONLY)	

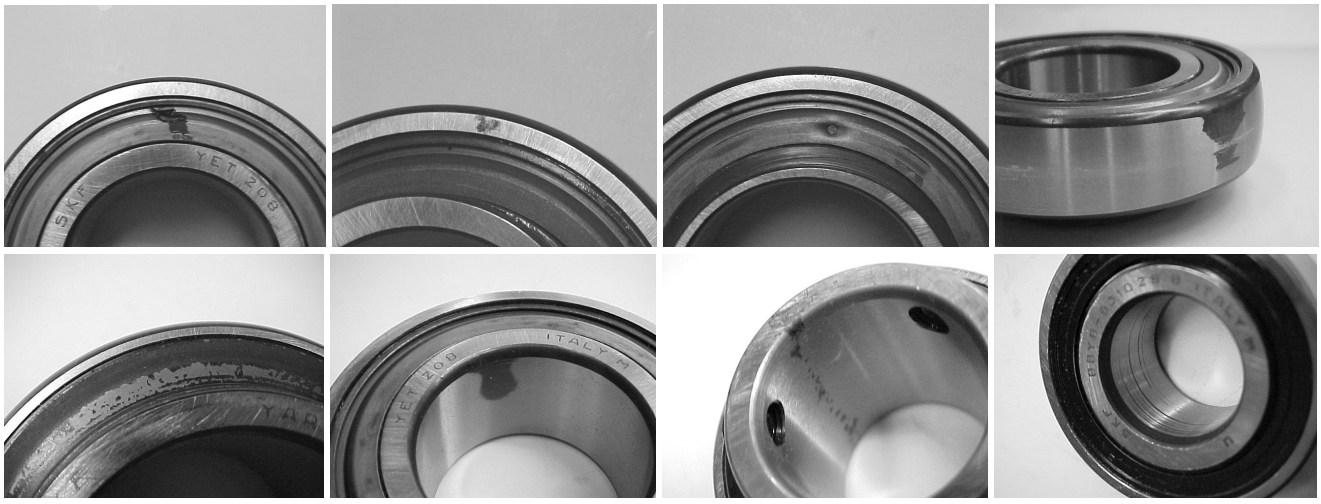

Figure 3: Examples of surface defects on ball bearings.

3.1 The camera configuration

The emphasis of this study is on the system configuration.

The possible camera configurations are summarized in Figure 4. An axial camera (with vertical axis) has a low field of direct view of the inner ring. A radial (horizontal) view (B) requires the product rotation or more than one camera for a complete acquisition. An intermediate position between the two cases (A) has a bad view of the inner or of the outer surface depending on the selected δ angle (Figure 4).

The use of mirrors increases the number of possibilities.

3.2 The product positioning

To reduce the processing time by maximizing the observed area in order to retrieve all the information necessary to perform the inspection from a single view, the following configuration has been selected:

1. the camera axis is coincident with the ball bearing axis;
2. a special device has been developed and a single image for each ball bearing side is processed. For a complete acquisition, a ball bearing is turned upside down.

The main elements of the positioning system are described in the next paragraphs. An image example is displayed in Figure 5.

The central mirror

To observe the inner surface of the ball bearing, a special conic mirror has been made, by chroming a polished steel cone. A secondary function of the cone is centering a ball bearing under the camera. The same cone can be used with different models in a certain size range. The cone angle ε is determined from the height h and inner diameter d_i of a ball bearing using the expression

$$\varepsilon = 180 - \arcsin\frac{d_i/2}{h} \qquad (1)$$

Only the lower half of the inner surface is inspected, considering that the ball bearing is turned upside down.

In (1), the whole inner surface is projected onto the cone surface and is visible by the camera because the cylindrical surface shrinkage towards the cone vertex is excessive. If the vertical spatial resolution of the inner cylindrical surface is not sufficient (in the case of high values of h), the ε angle of Figure 4 can be reduced accordingly, finding a compromise with the resolution reduction in the horizontal direction.

Of course, for all mirrors, regarding the light direction (γ angle of Figure 4), the incidence and the reflection angle (90 - γ) are the same. The ε angles of the cones made for the models SKF YET 208 and YAR 205 2F are respectively 140° and 160° (after precautionary rounding up).

The lateral mirrors

Additional lateral mirrors (four) are placed to observe the outer surface of the ball bearing that are parallel to the camera axis. The four mirrors position is adjustable in the radial direction to fit different ball bearing models.

Two lateral mirrors instead of four are able to cover half of the outer surface of the ball bearing each, but the distortion on the extreme sectors is excessive. With trigonometric relations it can be verified that the surface shrinkage is less than 37% in a central sector of 90° and it is over 58% in the two extreme sectors of 45°. In addition, the shrinkage in these areas is not constant, but it increases towards the extreme areas, which become practically not visible. Using four lateral mirrors, the surface shrinkage is limited to 37%, as explained above.

The optimal mirrors angle with respect to the horizontal plane is close to 45° in order to maximize the surface displayed.

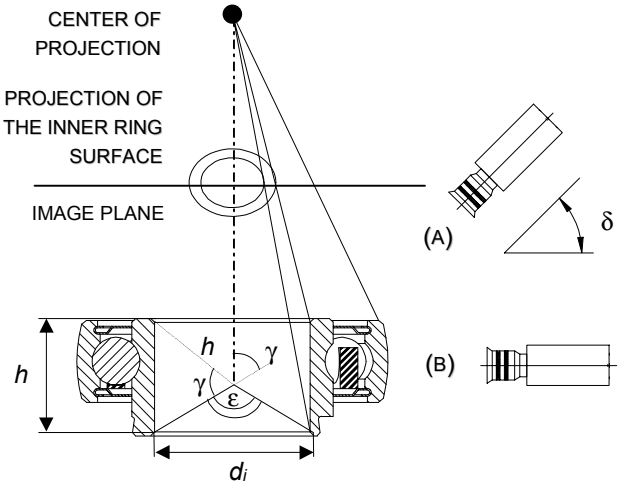

Figure 4: The available camera configurations: axial (vertical), inclined (A), and radial (B). The central conic mirror angle ε, is displayed as a function of the ball bearing height h and inner diameter d_i

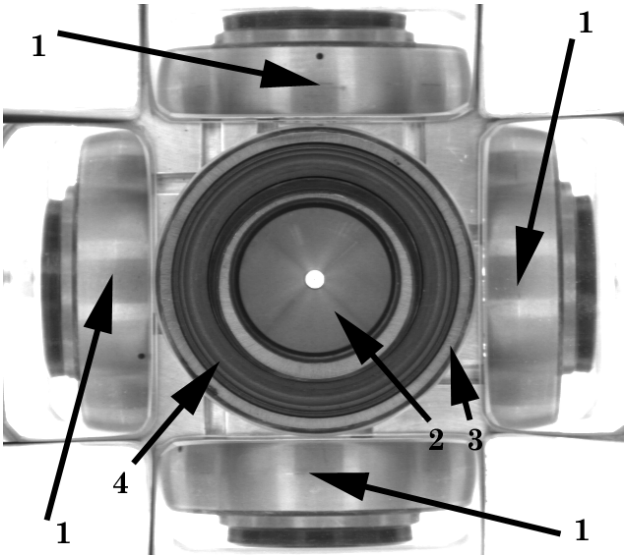

Figure 5: The surfaces inspected: (1) surfaces projected on the lateral mirrors; (2) surface projected on central conic mirror; (3) plane faces; (4) flinger. The small square at the top right of the ball bearing shows the reference area belonging to the positioning system.

3.3 The acquisition system

The camera

A monochrome camera (from IVC, model 800BC) has been selected considering that, in this kind of applications, the color information is usually not relevant. The required system resolution is 1 mm, because smaller defects have a negligible impact on the esthetic and functional features of ball bearings.

The CCD camera resolution is 768×576 pixel at 8 bit. Considering a field of view of about 150 mm, including the lateral mirrors of the positioning system, the nominal resolution is about 0.25 mm.

The optical system

The camera is equipped with a telecentric lens, from Kenko, model KCM-105T 55 mm, with a nominal distortion of 1%. The main benefit of this lens is that the perspective effect is virtually eliminated within the operative range.

3.4 The lighting system

The main problem concerned with lighting is that, with the system configuration selected, all surfaces, which have different curvatures and inclinations, are grabbed simultaneously. Distributes lighting reduces concentrated reflexes on the curved metal surfaces. Several configurations have been tested and assessed by comparing the light intensity of surface areas with and without defects.

Four 3 W 6 V DC lamps have been used. Indirect lighting is obtained by reflection on the surrounding white walls, whose function is also the isolation from the environmental light.

4 THE DEVELOPED ALGORITHMS AND SOFTWARE

The defect characterization (Table 1) has been the input for the implementation of the vision algorithms. In the main program interface, the control areas extracted from the grabbed image (Figure 5) are shown. In the online phase, they are processed in parallel.

The developed algorithms are able to detect the presence of a defect and its position. The defect type recognition is not required at this stage. Regarding turning and grinding marks, a visual distinction is not possible, because it depends on the machining stock height.

Inspection of the outer spherical surface

Rust, grinding and turning marks appear as dark blots on the bright metal surface.

The blots available on the outer spherical surface are detected with the following sequence of image processing steps: binarization followed by closing to eliminate isolated pixels. A product is considered defective if the number of dark pixels is over a predefined threshold. This threshold is determined considering the area of the two or three lubrication holes (depending on the model), which are present on all products. Considering the position of lubrication holes (usually at 120°), the following conditions should also be satisfied:

1. only one blot is allowed on each lateral mirror (Figure 5);
2. no more than two or three blots total (depending on the model) are allowed.

Inspection of the flingers

In general, the flingers are seen as an elliptic ring, for the change of the image aspect ratio during acquisition. For the inspection, three methods are possible:

- fixed control area and image rotation;
- fixed control area and ball bearing rotation;
- elliptic ring control area.

The last one is the fastest, because it can be performed in a single step. Defects are found as described in the previous paragraph, in the rectangular control area (outer rectangle in Figure 5) containing the elliptic ring. Their position is compared with the equations of the inner and

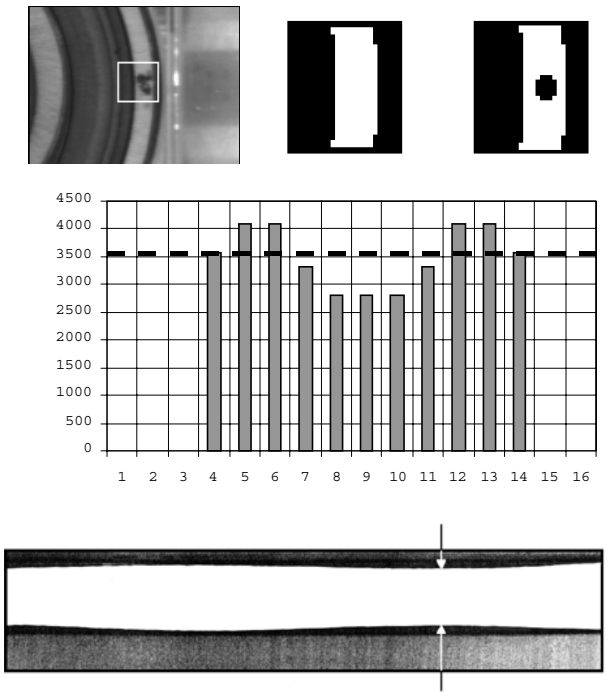

Figure 6: Detail of a defect on the plane face of the outer ring of a ball bearing. The control area is outlined (top, left). In the top right, the binarized control area is displayed in the case of absence and presence of a defect. The graph (center) shows the light intensity profile with a defect. In the bottom, an example of irregular intersection between the plane and the spherical surfaces is also shown.

of the outer boundary ellipses.

Inspection of the inner and outer ring plane faces

The plane faces have the same elliptic shape of flingers but they have a smaller size, about 11 pixels. The whole elliptic ring corresponding to the plane face is divided in smaller control areas where the plane face can be assumed as rectangular (Figure 6, top). Defects are detected by calculating the light intensity profiles, which is the addition of the pixel values in all columns of the control area, after binarization to enhance the defect presence. The number of consecutive column profiles that are below a predefined threshold is related to the presence of a defect. An example of graph is shown in Figure 6, center. With this method, a defective intersection between the plane and the outer spherical surface (Figure 6, bottom) can also be detected.

Inspection of the inner cylindrical surface

Considering that this surface, projected in the conic mirror, is observed as an elliptic ring, the same method described for flingers is used from the same control area (Figure 5).

Lubrication holes may also be present on the inner surface, like on the model SKF YAR 205 2F (Figure 7). In this case the following information are included in the algorithm:

1. their distance from the plane faces;
2. their angular distance (120°).

For the inspection, all the pixels belonging to the blots detected are sorted in polar coordinates and for each of them two conditions are then checked:

1. their radial position should be between the minimum and the maximum radius allowed for the lubrication holes;
2. the angular distance between two successive non-contiguous pixels with the same radius should correspond to the limits indicated in Figure 7 for the α and β angles.

Report generation

If any of the above algorithms finds a defect, a report is generated, which includes the defect type, and the date and time. This information can be used for quality assurance purposes, in order to find a correlation with the actual shift and with the process variables.

5 THE HARDWARE AND SOFTWARE CALIBRATION

The system setup for ball bearings of different size requires the installation of different conic mirrors and the adjustment of the lateral mirrors.

In general, the system calibration after the installation and production changes strongly influences the inspection algorithm performance, for this reason detailed procedures have been defined.

Figure 5 displays an example of grabbed image with the control areas inspected by the developed algorithms. It is necessary to manually adjust the size and position of the control areas after the initial system setup and for production changes to inspect different ball bearing models. The elliptic control areas for the flingers and the inner cylindrical surface are determined from the main axes, which are parallel to the image sides.

Interactive software has been implemented to fine-tune each control area. The control area width of the lateral mirrors is determined by the selected view angle discussed in Chapter 3.2.

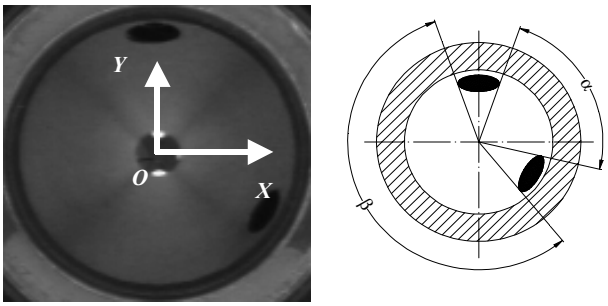

Figure 7: Top view of the conic mirror reflecting the innner cylindrical surface of the ball bearing, model SKF YAR 205 2F. The two lubrication holes, shown as dark blots at 120°, are visible.

Also the optimal lens aperture can be selected interactively. A reference area belonging to the positioning system is used (Figure 5). The light intensity of areas belonging to the ball bearing have shown a variability of more than 10%, which is not acceptable. The lens aperture is manually changed until the maximum of the histogram of the gray levels of the selected reference area reaches a pre-defined value (in our tests, 173). In addition, for each product, the status of the reference area is checked for errors.

The position of the reference control area is determined automatically, after the control area containing the outer plane face (Figure 5, n. 3) has been selected.

Considering that the observed area is square, the zoom is determined by fitting the view field within the short side of the image.

6 RESULTS

The proposed system has been tested with about 50 ball bearings, which were rejected out of 40,000 products inspected manually, representing all the defect classes indicated in Table 1.

Preliminary tests have been carried out to assess the algorithm robustness with respect to erroneous positioning and light changes.

The conic mirror performs the product centering on the positioning system. Manual loading tests have shown that it satisfactorily satisfies this task. This implies that a low accuracy will be required for the design of an automatic loading device.

Considering that the inspection algorithms are based on the absolute measurement of gray levels, light intensity changes have a strong influence on the system performance. In fact, light reductions determined the rejection of good products, and, inversely, over exposures did not allow the detection of defects. This shows the importance of the lens aperture setting, described in the previous chapter.

Two defect types of small size were not detected: hammering on flingers and rust traces.

Hammerings on flingers

Hammerings are critical because, depending on their depth, they may interfere with rolling. The defect shape suggests integrating a structured-light source to enhance its presence. An alternative consists in adding another probe in the station for the presence detection of screws.

Rust traces

The main problem regarding the small rust traces is that they are clearly visible on color images, but after conversion in grayscale their light intensity becomes

similar to that of the surrounding metal surface. An analysis of the causes producing this defect has shown that it is due to the improper packaging for the transportation from the supplier: when the rust depth exceeds the machining stock height, it is not completely removed in the grinding operation. By pointing out the cause of this defect, it has been reduced by the corrective action indicated.

7 THE SYSTEM ENGINEERING

A linear camera, with the CCD axis parallel to the radial direction, is more suitable for the system engineering, because it is well known that it is much easier to have repeatable lighting conditions, especially on curved surfaces. Regarding the system configuration, the good algorithm performance, also with more difficult lighting, suggests keeping the same camera position and rotating the ball bearing by 360°. In this case, the conic mirror can be replaced with a simpler centering system and a flat adjustable mirror. Turning the ball bearing upside down will be still necessary.

The static approach with a matrix camera has the benefit to reduce the acquisition time. The developed algorithms are suitable for both cases because they take advantage of the axial symmetry of ball bearings.

The metal surface reflexes have been minimized using multiple sources of indirect lighting.

The readability of markings was not investigated. OCR technology is available to be integrated in the system.

The positioning system developed is suitable to be installed directly on the line. Its main features are: low number of parts, standard components, no wear and tear (for the static configuration). The required space (less than 0.15 m^2 and 5 kg for the positioning system) is lower than that of the present manual inspection station (about 2 m^2). Its has been successfully tested with two very different ball bearings models. For the proper system interfacing on the line, the uploading and selective downloading of good and rejected products still needs to be studied.

8 SUMMARY

A detailed analysis of the controls on an automatic assembly line has been performed. The final visual inspection is the only manual operation and its performance can be improved with artificial vision.

The visual inspection of mechanical parts is state of the art. The main innovations of the developed system are:

1. the special configuration of the positioning system. The accessibility of all parts in a single view has been optimized with a mirror-based method;
2. the developed algorithms take advantage of the axial symmetry of ball bearings and are suitable both for the implementation with a matrix and a line CCD camera, discussed in the paper.

The system described, which also has a user-friendly interface, has been able to recognize most defects in off-line tests. The cycle time is 6 s, as required for the on-line application (the standard SKF cycle time).

9 ACKNOWLEDGMENTS

The authors wish to thank the management and the staff from SKF Industries & Co. Ltd., unit of Massa (Italy) involved in this project, in particular: Ing. Marco Ghignoli (director), Ing. Alberto Pieroni, and Ing. Ugo Moretti.

Ing. Emanuele Donati is gratefully acknowledged for his contribution to this study.

Support from the technical staff of the Department of Mechanical, Nuclear and Production Engineering, University of Pisa, is acknowledged.

10 REFERENCES

[1] Santochi, M., Dini, G., 1998, Sensor Technology in Assembly Systems, Annals of the CIRP, 47/2:1-22.

[2] Tonshoff, K., Janocha, H., Seidel, M., 1988, Image Processing in a Production Environment, Annals of the CIRP, 37/2:579-590.

[3] Lanzetta, M., Santochi, M., Tantussi, G., 1999, Computer-Aided Visual Inspection in Assembly, Annals of the CIRP, 48/1:21-24.

[4] Lanzetta, M., 1998, The Quality Control of Critical Assembly Components: Visual Inspection of O-rings, 2nd Int. Conf. on Planned Maintenance, Reliability and Quality, Oxford UK, 132-137.

[5] Lanzetta, M., Tantussi, G., 1999, Vision System Calibration and Sub-Pixel Measurement of Mechanical Parts, 5th Int. Conf. on Advanced Manufacturing Systems and Technology, Udine Italy, Springer-Verlag, 695-702.

[6] Elbestawi, M.A., Bone, G.M., Tam, P.W., 1992, An Automated Planning, Control, and Inspection System for Robotic Deburring, Annals of the CIRP, 41/1:397-400.

[7] Furukawa, Y., Sakuma, H., 1992, Automatic Detection of Defects among Small Pins-Group – Inspection of Connector-Plug Pins by the Use of Image Processing Associated with Neural Network, Annals of the CIRP, 41/1:589-592.

[8] Komatsu, T., Uno, S., Inoue, M., Sekiguchi, S., 1987, Automatic Inspection System for Chip Electronic Parts on a Printed Circuit Board, Annals of the CIRP, 36/1:399-402.

[9] Mengel, P., Roth, N., Schwartz, P., 1992, Application of Advanced Data Processing Technology for Integrated Inspection in Electronics Assembly, Annals of the CIRP, 41/1:29-32.

[10] QTC SKF, 1999, MZU 120A Outlier Detection Unit.

[11] Axon Electrofotonica, 1998, Ball Bearing Automated Optical Inspection Station.

[12] Axon Electrofotonica, 1999, Automated Optical Inspection Sytem.

[13] Pfeifer, T. Wiegers, L., 1998, Adaptive control for the optimized adjustment of imaging parameters for surface inspection using machine vision, Annals of the CIRP, 47/1:487-490.

[14] Milutinovic, D.S., Milacic V.R., 1987, A model-based vision system using a small computer, Annals of the CIRP, 36/1:327-330.

[15] Lanzetta, M., 1997, The Introduction of a New Functionality in Existing Industrial Products: the Case of OCR in an Artificial Vision System, 10th Int. ADM Conf. «Design Tools and Methods in Industrial Engineering», Florence Italy, 301-310.

[16] MIL-Q-9858A standards, 1 October 1996.